Biogeosciences Discuss., https://doi.org/10.5194/bg-2018-91
Manuscript under review for journal Biogeosciences
Discussion started: 4 April 2018

Biogeochemical and microbiological evidence for methane-related archaeal communities at active submarine mud volcanoes on the Canadian Beaufort Sea slope

Dong-Hun Lee[1], Jung-Hyun Kim[2,*], Yung Mi Lee[2], Alina Stadnitskaia[3], Young Keun Jin[2], Helge Niemann[4], Young-Gyun Kim[5], Kyung-Hoon Shin[1,**]

[1]Department of Marine Sciences and Convergent Technology, Hanyang University, 425-791 Ansan, South Korea

[2]KOPRI Korea Polar Research Institute, 406-840 Incheon, South Korea

[3]European Council for Maritime Applied R&D, Rue Marie de Bourgogne 52-54, B-1000 Bruxelles, Belgium

[4]NIOZ Royal Netherlands Institute for Sea Research, Department of Marine Microbiology and Biogeochemistry, and Utrecht University, NL-1790 AB Den Burg, The Netherlands

[5]Research Institute for Earth Resources, Kangwon National University, 24341, Chuncheon, South Korea

[*]Corresponding author:
Tel.: +82 32 760 5377
jhkim123@kopri.re.kr

[**]Corresponding author:
Tel.: +82 31 400 5536
shinkh@hanyang.ac.kr

Biogeosciences Discuss., https://doi.org/10.5194/bg-2018-91
Manuscript under review for journal Biogeosciences
Discussion started: 4 April 2018

Abstract

In this study, we report lipid biomarker patterns and phylogenetic identities of key microbes mediating anaerobic oxidation of methane (AOM) communities in active mud volcanos (MVs) on the continental slope of the Canadian Beaufort Sea. The enriched $\delta^{13}C$ values of total organic carbon (TOC) as well as lipid biomarkers such as archaeol and biphytanes (BPs) relative to $\delta^{13}C_{CH4}$ values suggested that the contribution of AOM-related biomass to sedimentary TOC was in general negligible in the Beaufort Sea MVs investigated. However, the $\delta^{13}C$ values of *sn*-2- and *sn*-3-hydroxyarchaeol were more negative than CH_4, indicating the presence of AOM communities, albeit in a small amount. The ratio of *sn*-2-hydroxyarchaeol to archaeol and the 16S rRNA results indeed indicated that archaea of the ANME-2c and ANME-3 clades were involved in AOM. Further studies are needed to investigate the diversity and distribution of AOM communities and to characterize their habitats in the uppermost surface sediments of Beaufort Sea MV systems.

Keywords: Arctic, Beaufort Sea, submarine mud volcano, methane, anaerobic oxidation of methane (AOM), lipid biomarkers, 16S rRNA

Biogeosciences Discuss., https://doi.org/10.5194/bg-2018-91
Manuscript under review for journal Biogeosciences
Discussion started: 4 April 2018

1 Introduction

Pingo-like features (PLFs) are rounded positive-relief mounds that have been discovered in permafrost and hydrate-bearing regions onshore and offshore across the Arctic (e.g. Shearer et al., 1971; Walker et al., 1985; Grosse and Jones, 2011; Serov et al., 2017). Submarine PLFs were first discovered on the Beaufort Shelf in 1969 by hydrographers aboard the C.C.G.S. John A. MacDonald, a Canadian Coast Guard icebreaker (Shearer et al., 1971). During the course of the southern Beaufort Sea mapping program that followed, numerous PLFs were found ranging from 20 to 980 m in diameter, 41 to 311 m in width, and 1 to 50 m in height in water depths of 20 to 200 m (Blasco et al. 2013 and references therein). Submarine PLFs can be classified into five categories of origin: submarine-formed true pingos, mud volcanoes, diapirs, relict topography and slump features (Blasco et al., 2006). The PLFs on the Beaufort Sea shelf appear to be geographically controlled by the presence of submerged permafrost (Paull et al, 2007). The present hypothesis for the formation of submarine PLFs is linked to the dissociation of methane gas hydrate as a consequence of the flooding of relatively warm marine waters over cold permafrost areas during the Holocene (Paull et al., 2007; Serov et al., 2017). Eruptions of submarine PLFs may supply methane to the overlying water column and ultimately to the atmosphere (e.g. Feseker et al., 2014). Submarine PLFs are therefore of considerable interest in global warming scenarios, since methane is a greenhouse gas that is >20 times more potent than carbon dioxide (Wuebbles and Hayhoe, 2002; Etmian et al., 2016).

Over the outer Beaufort Shelf, PLFs were discovered in water depths of ~282 m, ~420 m, and ~740 m during the multibeam bathymetric mapping surveys conducted in 2009 and 2010 (Campbell et al., 2009; Saint-Ange et al., 2014). These PLFs were interpreted as being mud volcanoes (MVs) associated with the extrusion of gas and water-saturated fine-grained

sediment (e.g. Kopf, 2002); they were designated by their water depths (Blasco et al., 2013; Saint-Ange et al., 2014). Previous investigations of MVs in the Beaufort Sea based on sediment cores, detailed mapping with an autonomous underwater vehicle (AUV), and exploration with a remotely operated vehicle (ROV) showed that these MVs are young, active edifices characterized by ongoing eruptions (Paull et al., 2015). The gas ascending via these MVs consists of >95 % CH_4 with $\delta^{13}C_{CH4}$ values of –64 ‰, indicating a microbial source (Paull et al., 2015). Colonized siboglinid tubeworms and white bacterial mats, the first evidence of living chemosynthetic biological communities, were reported from MV420 (Paull et al., 2015). Although detailed bathymetric mapping and methane-rich fluid dynamics are comparably well invesitgated, the biogeochemical processes related to the archaeal-associated anaerobic oxidation of methane (AOM) have not yet been investigated in the MV systems of the Beaufort Sea.

In this study, we investigated three sediment cores recovered from active MVs on the continental slope of the Canadian Beaufort Sea during the ARA05C expedition with the R/V Araon in 2014. Bulk chemical compounds, specific archaeal lipids and their stable carbon isotopic compositions were investigated in order to characterize the anaerobic oxidation of methane (AOM) communities in the MV sediments. We compared biogeochemical parameters with the diversity of archaea. Using integrated lipid and nucleic acid analyses, our study sheds light on the specific archaeal communities involved in AOM at active MVs in the Canadian Beaufort Sea.

2 Material and Methods

2.1 Sample collection

Three sediment cores were taken using a gravity corer during the ARA05C expedition

with R/V Araon, the South Korean icebreaker, in August 2014 in the Canadian Beaufort Sea (Fig. 1A-C). Core ARA05C-10-GC (70°38.992'N, 135°56.811'W, 282 m water depth, 221 cm core length), core ARA05C-01-GC (70°47.342'N, 135°33.952'W, 420 m water depth, 272 cm core length), and core ARA05C-18-GC (70°48.082'N, 136°05.932'W, 740 m water depth, 300 cm core length) were retrieved from the active MV sites MV282, MV420 and MV740, respectively. Upon recovery, all three sediment cores were observed to expand and bubble profusely. The retrieved sediment cores were split, lithologically described, and subsampled for the analysis of bulk elements, lipid biomarkers and 16S rRNA gene sequences on board. After subsampling, sediment samples were immediately deep-frozen and stored at –20℃ for geochemical analyses and at –80℃ for microbial analyses.

2.2 Bulk geochemical analysis

Sediment samples were freeze-dried and homogenized using an agate mortar prior to bulk geochemical analyses. Sediment samples (~1 g) were treated with 8 mL 1N HCl to remove carbonates prior to the analyses. The total organic carbon (TOC) content and its isotopic composition were measured using an elemental analyzer (EuroEA3028, Eurovector, Milan, Italy) connected to an isotope ratio mass spectrometer (Isoprime, GV instruments, Manchester, UK). The stable carbon isotopic values of TOC ($\delta^{13}C_{TOC}$) were reported in standard delta (δ) notation relative to Vienna Pee Dee Belemnite (VPDB) scale in per mill. The analytical errors (standard deviations of repeatd measurments of the internal standard IAEA CH_6) were smaller than ±0.1 wt.% for TOC, and ±0.1 ‰ for $\delta^{13}C_{TOC}$.

2.3 Lipid extraction and purification

The homogenized sediment samples (ca. 10 g) were extracted with an accelerated solvent

extractor (Dionex ASE 200, Dionex Corporation, Sunnyvale, CA) using a solvent mixture of 9:1 (v:v) dichloromethane (DCM) to methanol (MeOH) at a temperature of 100℃ and a pressure of 7.6×10^6 Pa. The total lipid extract was dried over anhydrous Na_2SO_4 and was treated with tetrabutylammonium sulfite reagent to remove elemental sulfur. The aliquot was chromatographically separated into apolar and polar fractions over an Al_2O_3 (activated for 2 h at 150℃) column with solvents of increasing polarity. The apolar fraction was eluted using hexane:DCM (9:1, v:v), and the polar fraction was recovered with DCM:MeOH (1:1, v:v) as eluent. After column separation, 40 µl of 5α-androstane (10 µg/mL) were added to the apolar fraction as an internal standard. The polar fraction was divided into two splits, to which either C_{22} 7,16-diol (10 µg/mL) or C_{46} GDGT (10 µg/mL) was added as an internal standard. The half of the polar fraction containing C_{22} 7,16-diol was dried and silylated with 25 µL N,O-bis(trimethylsilyl)trifluoroacetamide (BSTFA) and 25 µL pyridine before being heated at 60℃ for 20 min to form trimethylsilyl derivatives. The half of the polar fraction containing C_{46} GDGT was re-dissolved by sonication (5 min) in hexane:isopropanol (99:1, v:v) and then filtered with a 0.45-µm PTFE filter. Afterwards, an aliquot of the filtered fraction was treated with HI following the procedure described by Kaneko et al. (2011) in order to cleave ether bonds from glycerol dialkyl glycerol tetraethers (GDGTs), thereby releasing biphytanes (BPs) which can be analyzed by a gas chromatography (GC).

2.4 Identification and quantification of lipid biomarkers

All apolar and polar fractions were analyzed using a Shimazu GC (Shimazu Corporation, Kyoto, Japan) equipped with a splitless injector and a flame ionization detector for compound quantification. A fused silica capillary column (CP-sil 5 CB, 25-m length, 0.32-mm i.d., and 0.12-µm film thickness) was used with He (1.3 mL/min) as a carrier gas. The samples were

injected under constant flow at an initial oven temperature of 70℃. The GC oven temperature was subsequently raised to 130℃ at a rate of 20℃/min, and then to 320℃ at 4℃/min with a final hold time of 15 min. Concentrations were obtained by comparing the peak area of each compound with that of 5α-androstane for the apolar fraction and C_{22} 7,16-diol for the polar fraction. Compound identifications for the apolar, silylated and BP polar fractions were conducted using a Shimazu GC connected to a GCMS-QP2010 mass spectrometer (MS) (Shimazu Corporation, Kyoto, Japan) operated at 70 eV (cycle time of 0.9 s, resolution of 1000) with a mass range of *m/z* 50–800. The samples were subjected to the same temperature conditions and capillary column described for GC analysis. Molecular structures were determined by comparing their mass spectral fragmentation patterns and retention times with previously published data.

An aliquout of the filtered polar fractions was analyzed by high-performance liquid chromatography–atmospheric pressure positive ion chemical ionization–mass spectrometry using an Agilent 6120 Series LC/MSD SL system (Agilent Technologies, Santa Clara, CA) equipped with an auto-injector and Chemstation chromatography manager software. Separation was achieved on two UHPLC silica columns (2.1 × 150 mm, 1.7 μm), fitted with 2.1 × 5 mm pre-column of the same material and maintained at 30℃. Injection volumes varied from 1 μL. GDGTs were eluted isocratically with 82% A and 18% B for 25 min, followed by a linear gradient to 35% B over 25 min, then to 100% B over 30 min, and finally maintained for 20 min, where A = hexane and B = hexane:2-propanol (90:10, v:v). The flow rate was 0.2 mL/min, with a total run time of 90 min. After each analysis, the column was cleaned by back-flushing hexane:2-propanol (90:10, v:v) at 0.2 mL/min for 20 min. Conditions for APCI-MS were as follows: nebulizer pressure 60 psi, vaporizer temperature 400℃, drying gas (N_2) flow 6 mL/min and temperature 200℃, capillary voltage –3.5 kV,

corona 5 µA (~3.2 kV). Detection was achieved in single ion monitoring of $[M + H]^+$ ions (dwell time 35 ms), as described by Schouten et al. (2007). GDGTs were quantified by integrating peak areas and using the internal standard according to Huguet et al. (2006).

2.5 Compound-specific stable carbon isotope analysis

The $\delta^{13}C$ values of selected compounds were determined by GC/combustion/isotope ratio mass spectrometry (GC-C-IRMS), as described by Kim et al. (2017). An IRMS (Isoprime, GV Instruments, UK) was connected with a GC (Hewlett Packard 6890 N series, Agilent Technologies, Santa Clara, CA) via a combustion interface (glass tube packed with copper oxide (CuO), operated at 850°C). The samples were subjected to the same temperature conditions and capillary column described for the GC and GC-MS analyses. Calibration was performed by injecting several pulses of reference gas CO_2 of known $\delta^{13}C$ value at the beginning and the end of each sample run. Isotopic values are expressed as $\delta^{13}C$ values in per mil relative to the Vienna-PeeDee Belemnite (VPDB). The $\delta^{13}C$ values were further corrected using a certified isotope standard (Schimmelmann alkane mixture type A6, Indiana University). The correlation coefficients (r^2) of the known $\delta^{13}C$ values of certified isotope standards with the average values of the measured samples were higher than 0.99. In the case of silylation of alcohols for $\delta^{13}C$ measurement, values need to be corrected for the addition of an $Si(CH_3)_3$ group during the derivatization procedure. In this study, the $\delta^{13}C$ value of the BSTFA was determined (–19.3±0.5 ‰). In order to monitor the accuracy of the measurements, standards with known $\delta^{13}C$ values were repeatedly analyzed every 5–6 sample runs. Standard deviations of carbon isotope measurements were generally better than ±0.4 ‰, as determined by repeated injections of the standard.

2.6 Genomic DNA extraction and amplification of 16S rRNA genes

Genomic DNA was extracted from approximately 1-2 g of sample using the FastDNA Spin Kit for Soil (Q-Biogene, Carlsbad, CA, USA). 16S rRNA gene was amplified by polymerase chain reaction (PCR) using the 8F (3-CTCAGAGTAGTCCGGTTGATCCYGCCGG-5') / 519R (3'-ACAGAGACGAGGTDTTACCGCGGCKGCTG-5') primers with barcodes for archaeal community analysis. PCR was carried out with 30 μL of reaction mixture containing DreamTaq Green PCR Master Mix (2×) (Thermo Fisher Scientific, Waltham, MA, USA), 1 μL of 5 μM primers, and 4 μL of genomic DNA. The PCR procedure included an initial denaturation step at 94°C for 3 min, 30 cycles of amplification (94°C for 1 min, 55°C for 1 min, and 72°C for 1.5 min), and a final extension step at 72°C for 5 min. Each sample was amplified in triplicate and pooled. PCR products were purified using the LaboPass purification kit (Cosmogenetech, Seoul, Korea). Due to PCR failure for samples below 0.6 m in the MV740 sample, these samples were not included in further analysis.

2.7 Archaeal community and phylogenetic analysis

Sequencing of the 16S rRNA amplicon was carried out by Chun Lab (Seoul, South Korea) using a 454 GS FLX-Titanium sequencing machine (Roche, Branford, CT, USA). Preprocessing and denoising were conducted using PyroTrimmer (Oh et al., 2012). Sequences were processed to remove primer, linker, and barcode sequences. The 3′ ends of sequences with low quality values were trimmed when the average quality score for a 5-bp window size was lower than 20. Sequences with ambiguous nucleotides and those shorter than 250 bp were discarded. Chimeric reads were detected and discarded using the *de novo* chimera detection algorithm of UCHIME (Edgar et al., 2011). Sequence clustering was

performed using CLUSTOM (Hwang et al., 2013) with a 97 % similarity cutoff. Taxonomic assignment was conducted for representative sequences of each cluster by EzTaxon-e database search (Kim et al., 2012). Raw reads were submitted to the the National Center for Biotechnology Information (NCBI) Sequence Read Archive (SRA) database (accession number PRJNA433786).

Because 16S rRNA gene phylogenies of methanomicrobial operational taxonomic units (OTUs) comprised more than 1 % (relative abundance), sequences were aligned with those of *Methanomicrobia* using jPhydit. A phylogenetic tree was constructed using the maximum-likelihood algorithm (Felsenstein et al., 1980) with MEGA 6 (Tamura et al., 2013). The robustness of the tree topologies was assessed by bootstrap analyses based on 1,000 replications of the sequences.

3 Results

3.1 Bulk geochemical and microbial lipid analyses

Bulk geochemical data are summarized in Supplementary Information Table S1. Overall, the TOC contents of core sediments from MV282, MV420 and MV740 ranged from 1.2–1.5 wt.%, 1.0–1.3 wt.%, and 1.1–1.3 wt.%, respectively, but did not vary systematically with core depths. Similarly, $\delta^{13}C_{TOC}$ values in MV282, MV420 and MV740 showed little variation, with average values of –26.3±0.07 ‰, –26.2±0.05 ‰, and –26.3±0.06 ‰, respectively.

In polar component analysis, the isoprenoid dialkyl glycerol diethers (DGDs) archaeol (2,3-di-*O*-phytanyl-*sn*-glycerol) and *sn*-2-hydroxyarcaheol (2-*O*-3-hydroxyphytanyl-3-*O*-phytanyl-sn-glycerol) were identified in all three MVs (Fig. 2); their concentrations were 0.03–0.09 μg/g and 0.01–0.13 μg/g, respectively (Fig. 3, see also Table S1). *Sn*-3-hydroxyarchaeol was only identified in MV282 and MV420; concentrations were 0.01–0.08

μg/g (Fig. 3, see also Table S1). Among non-isoprenoid DGDs, DGD (If) with *anteiso* pentadecyl moieties attached at both the *sn*-1 and *sn*-2 positions was identified in three MVs. The concentrations of non-isoprenoid DGD (If) ranged from 0.06 to 0.25 μg/g (Fig. 3, see also Table S1). Isoprenoid glycerol dialkyl glycerol tetraethers (GDGTs) containing 0 to 3 cyclopentane moieties (GDGT-0 to GDGT-3) and crenarchaeol which, in addition to 4 cyclopentane moieties, contains a cyclohexane moiety, were detected in all samples investigated (Fig. 4). Overall, the isoprenoidal GDGTs were dominated by GDGT-0 and crenarchaeol, with concentrations of 0.02–0.19 μg/g and 0.02–0.25 μg/g, respectively, whereas GDGT-1 and GDGT-2 showed much lower concentrations (≤0.02 μg/g) in the three MVs. In apolar component analysis, we could not detect the irregular, tail-to-tail linked isoprenoid acyclic C_{20} (2,6,11,15-tetramethylhexadecane, crocetane) and C_{25} (2,6,10,15,19-pentamethylicosane, PMI) hydrocarbons.

At the three MVs, the $\delta^{13}C$ values of archaeol and *sn*-2-hydroxyarchaeols ranged from –79.8 to –38.5 ‰ and from –113.9 to –82.1 ‰, respectively (Fig. 3, Table S1). The $\delta^{13}C$ values of *sn*-3-hydroxyarchaeol were as low as –93.1 ‰. The $\delta^{13}C$ values of the non-isoprenoid DGD (If) varied between –46.9 and –31.9 ‰. The $\delta^{13}C$ values of BPs derived from the isoprenoid GDGTs ranged from –63.4 to –16.7 ‰. The $\delta^{13}C$ values of BP-1 (on average –51.0 ‰) were slightly more depleted than those of BP-0 (on average –34.2 ‰), BP-2 (on average –28.3 ‰) and BP-3 (on average –27.5 ‰).

3.2 Depth profile of archaeal classes

Archaeal diversity among pyrosequencing reads was relatively low in the investigated Beaufort Sea MVs (Supplementary Information Table S2 and Fig. S2). Eight different archaeal classes were detected; five of these groups belong to the Euryarchaeota and three

belong to the Crenarchaeota and the Thaumarchaeota. The archaeal classes detected were Miscellaneous Crenarchaeotal Group (MCG)_c, Methanomicrobia, SAGMEGMSBL_c, Thermoplasmata, Marine Benthic Group B (MBGB)_c, MHVG3_c, Marine Group 1a_c, and Marine Group 1b_c. MCG_c of the phylum Crenarchaeota was the most dominant archaeal class at the three MVs at a range of depths, with the exception of the surface of MV420, accounting for 39.7 to 99.2 % of the toal archaeal sequences. In contrast to the archaeal communities below 0.3 m in MV282 and 1.1 m in MV420, which were dominated by MCG_c, shallow archaeal communities at depths of 0.0–0.2 m at MV282, 0.1–0.7 m at MV420, and 0.1–0.6 m at MV740 had different compositions in the MVs. The class *Methanomicrobia* represented a relatively high proportion (up to 20.9 %) in these shallow depths at all three MVs.

4 Discussion

4.1 Evidence of AOM in Beaufort Sea mud volcanoes

Recently, MVs have been identified on the continental slope of the Canadian Beaufort Sea, and active methane seepages have been documented at the MV282, MV420, and MV740 sites (see Fig. 1; Paull et al., 2015). Upon core recovery, all three cores retrieved from these active MVs were noticeably gas-charged, i.e. developing gas-filled gaps within the cores due to gas expansion (Fig. 1D). Sediments were mainly composed of homogeneous brown and dark gray silty clay. Mousse-like textures were observed in core ARA05C-10-GC and core ARA05C-01-GC, representing deformation related to gas expansion (Paull et al., 2015 and references therein). We also found gas hydrates, i.e. about ≤2 cm thick isolated veins at the bottom (230 to 300 cm) of core ARA05C-18-GC. Several of the lines of evidence mentioned above suggest that interstitial gas is saturated near the seafloor of the investigated edifices

(Paull et al., 2015). However, organic carbon contents and $\delta^{13}C_{TOC}$ values of the three sediment cores investigated spanned a narrow ranges of 1.2±0.1 wt.% and –26.4±0.6 ‰, respectively (see Table S1 and Fig. S1), without the negative isotopic excursion that has often been associated with methane-derived biomass from AOM in MVs (e.g. Haese et al., 2003; Werne et al., 2004). Hence, our bulk geochemical data suggest that the contribution of AOM-related biomass to sedimentary TOC is rather low at the MVs investigated.

AOM in marine sediments typically proceeds with sulfate as the terminal electron acceptor (Boetius et al., 2000, Reeburgh, 2007; Knittel et al., 2009; James et al., 2016), although recent research also found indications for AOM with electron acceptors other than sulfate, i.e. oxidised Mn and Fe species (Beal et al., 2009) or nitrate/nitrite (Haroon et al., 2013). The key microbial communities involved in sulfate-dependent AOM are anaerobic methane oxidisers (ANMEs) in association with sulfate reducing partner bacteria (Knittel et al., 2009, Wegener et al., 2008), although ANMEs may also mediate sulfate-dependent AOM without bacterial partners (Milcuka et al., 2012). AOM with alternative electron acceptors in marine settings is probably mediated by specialised ANMEs (Beal et al., 2009; Haroon et al., 2013), but it remains unclear in how far potential partner bacteria are involved in these processes. At the mud volcanoes investigated here, we found indications for methane-sulfate transition zones (based on sulfate penetration depth) at 0.20 (MV270), 0.20 (MV420) and 0.45m bsf (MV740) with correspondingly elevated abundancies of sulfate-dependent AOM communities and their lipid biomarkers (see discussion on AOM communities in sediments in section 4.2). Our data thus suggest AOM with sulfate as the terminal electron acceptor.

As a result of stable carbon isotope fractionation during AOM, AOM-derived biomass (including lipids) are generally depleted in ^{13}C compared to the $\delta^{13}C$-values of source methane (Whiticar, 1999). Consequently, the $\delta^{13}C$-values of AOM-derived lipids are widely

used to identify AOM in paleo (e.g. Zhang et al., 2003; Stadnitskaia et al.,2008b; Himmler et al., 2015) and modern seep settings (e.g. Hinrichs and Boetius, 2002; Niemann et al., 2005; Chevalier et al., 2011, 2014). Non-isoprenoid DGD (If), potentially a marker of sulfate-reducing bacteria (SRB) related to AOM (e.g. Pancost et al., 2001a; Werne et al., 2002), was detected throughout all three MV sediment cores (Fig. 3). The $\delta^{13}C$ values of the non-isoprenoid DGD (If) (–46.9 to –32.6 ‰) were however enriched relative to the ascending methane in the MVs (about –64 ‰, Paull et al., 2015). Hence, our $\delta^{13}C$ data of the non-isoprenoid DGD (If) are not directly supportive of the presence of SRB possibly involved in AOM.

Moreover, the isoprenoid GDGT distributions (Fig. 4) did not show a clear dominance of GDGT-2 over GDGT-0, indicative of the negligible contribution of Euryarchaeota related to AOM (e.g. Pancost et al., 2001b; Zhang et al., 2003; Niemann et al., 2005; Stadnitskaia et al., 2008a, b). The values of the GDGT-0/crenarchaeol (Liu et al., 2011), the GDGT-2/crenarchaeol (Weijers et al., 2011), and the methane index (Zhang et al., 2011) were also low, with ranges of 0.8–1.7, 0.1–0.2, and 0.2–0.4, respectively. The $\delta^{13}C$ values of BPs (Table S1) were generally more enriched than the $\delta^{13}C_{CH4}$ value of about –64 ‰ (Paull et al., 2015). These lines of evidence confirm that the isoprenoid GDGT inputs from methanotrophic archaea were low in the investigated sediments.

However, although the AOM contribution to the bulk sedimentary TOC pool is rather low, we identified *sn*-2-hydroxyarchaeol among isoprenoid DGDs in all three MV sediment cores as AOM-related biomarkers (Fig. 3). *Sn*-3-hydroxyarchaeol, an isomer of *sn*-2-hydroxyarchaeol (e.g. Pancost et al., 2000; Elvert et al., 2005; Niemann et al., 2005; Bradley et al., 2009), was also detected in MV282 but not in MV420 and MV740, except for at 0.7 m in MV420 (Fig. 3). The $\delta^{13}C$ values of *sn*-2-hydroxyarchaeol were more depleted than the

$\delta^{13}C_{CH4}$ values (about –64 ‰, Paull et al., 2015), with average $\Delta\delta^{13}C$ values of –35.5 ‰ in MV282, –33.8 ‰ in MV420, and –29.5 ‰ in MV740. Notably, the $\Delta\delta^{13}C$ values of *sn*-2-hydroxyarchaeol were slightly larger in MV282 than in other MVs. Similar to *sn*-2-hydroxyarchaeol, the $\delta^{13}C$ values of *sn*-3-hydroxyarchaeol in the MV sediments were in general more depleted than the $\delta^{13}C_{CH4}$ values. Accordingly, our $\delta^{13}C$ data of *sn*-2- and *sn*-3-hydroxyarchaeol are indicative of the presence of AOM in the Beaufort Sea MVs investigated.

Furthermore, the sulfate profiles of pore waters showed a steep gradient in the upper 0.5 m of cores in the investigated MVs (see Fig. S1) and siboglinid tubeworms closely related to *Oligobrachia haakonmosbiensis* as well as white bacterial mats were previously found at the summit of MV420 (Paull et al., 2015). The biogeochemical functioning of the chemosynthetic communities involved in methane oxidation in these MVs have not been constrained previously. However, the sibloginids can host methane and/or sulfide-oxidizing bacteria (e.g. Lösekann et al., 2008; Felden et al., 2010) and white bacterial mats at cold seeps are usually sulfur oxidisers (e.g. Niemann et al., 2005; Omoregie et al., 2009; Hovland et al., 2012). This implies that the chemosynthetic communities at MVs investigated here are fueled either by methane directly or by sulfide, one of the the endproducts of AOM. Hence, CH_4 is most likely, at least in small amounts, being oxidized near the seafloor, and our lipid data provide evidence for AOM in deeper sediments too.

4.2 AOM-related microbial communities in Beaufort Sea mud volcanoes

4.2.1 Chemotaxonomy

The composition of microbial lipids and their $\delta^{13}C$ values can be used to infer the chemotaxonomic composition of microbes involved in AOM (Niemann and Elvert, 2008 and references therein). Previously, three groups of anaerobic methanotrophic archaea (ANME-1,

ANME-2 and ANME-3) have been reported in diverse cold seep environments (Niemann and Elvert, 2008 and reference therein), which are related to methanogens of the orders *Methanosarcinales* and *Methanomicrobiales* (e.g. Boetius et al., 2000; Knittel et al., 2005; Niemann et al., 2006; Knittel and Boetius, 2009). Archaeol is ubiquitous in archaea, generally serving as an indicator of methanogenic archaea in a wide range of environments including MVs (e.g. De Rosa and Gambacorta, 1988; Koga et al., 1993, 1998; Pancost et al., 2011). In contrast, *sn*-2-hydroxyarchaeol has only been found in certain orders of methanogens such as *Methanosarcinales*, *Methanococcales*, *Methanopyrales*, *Thermoplasmatales*, *Sulfolobales* and *Methanomicrobiales* (e.g. Kushwaha and Kates, 1978; Koga et al., 1993, 1998; Koga and Morii, 2005), whereas s*n*-3-hydroxyarchaeol has been detected in *Methanosarcinales* (*Methanosaeta concilii*) and *Methanococcales* (*Methanococcus voltae*) (Ferrante et al., 1988; Sprott et al., 1993).

Blumenberg et al. (2004) showed that microbial mats dominated by ANME-2 at the cold seeps of the northwestern Black Sea contained higher amounts of *sn*-2-hydroxyarchaeol relative to archaeol, whereas archaeol was more abundant than *sn*-2-hydroxyarchaeol in microbial mats dominated by ANME-1. Consequently, the ratio of *sn*-2-hydroxyarchaeol to archaeol was proposed as a tool to distinguish ANME-1 (0–0.8) from ANME-2 (1.1–5.5). This ratio for ANME-3 (2.4) fell within the range of ANME-2 (Niemann et al., 2006; Niemann and Elvert, 2008). In our dataset, the concentration of *sn*-2-hydroxyarchaeol was generally slightly higher than that of archaeol in MV282, but lower in MV420 and MV740 (Fig. 3, see also Table S1). Accordingly, the *sn*-2-hydroxyarchaeol/archaeol ratio was between 1.3 and 1.8 in MV282, but below 0.7 for most of the samples from MV420 and MV740, except for at depths of 0.7 m (1.4) in MV420 and 0.4–0.6 m (0.9–1.1) in MV740 (Fig. 3, see also Table S1). This observation suggests that ANME-2 (or ANME-3) was

involved in AOM in MV282, whereas ANME-1 was probably involved in AOM in MV420 and MV740, except for at the depths mentioned above.

However, the $\delta^{13}C$ values of archaeol were on average –62.6 ‰ in MV282, –49.4 ‰ in MV420, and –54.3 ‰ in MV740, except for at 0.7 m in MV420 (–79.8 ‰). Hence, the $\delta^{13}C$ values of archaeol in most of the MV sediments appeared to be enriched in comparison to that of the ascending methane in the MVs (about –64 ‰, Paull et al., 2015), indicating an origin from methanogenesis rather than AOM. Hence, it appears that the ratio of *sn*-2-hydroxyarchaeol to archaeol was generally high in all investigated MVs, hinting a neglegible involvement of ANME-1 in AOM even in MV420 and MV740. Previous studies (e.g. Blumenberg et al., 2004; Stadnitskaia et al., 2008a, b) showed that GDGTs were mostly abscent in ANME-2-dominated settings, whereas GDGTs were detected in ANME-1-dominated settings with the predominance of GDGT-1 and GDGT2. Hence, a supporting evidence for the absence of ANME-1 in the investigated MVs can be found from the GDGT distributions (Fig. 4), showing a clear dominance of GDGT-0 and crenarchaeol over GDGT-1 and GDGT-2. Hence, our lipid data indicate that ANME-2 and/or ANME-3 are involved in AOM in the Beaufort Sea MVs investigated but not ANME-1. However, we could not detect crocetane, a diagnostic irregular isoprenoidal hydrocarbon for methanotrophic archaea associated with ANME-2 (Elvert et al., 1999) as well as PMIs which are structurly similar to crocetane produced by both ANME-2 and ANME-3 (Niemann and Elvert, 2008) so that further chemotraxonomic distinction of the dominant ANME groups can not be done.

4.2.2 Nucleic acid based phylogeny

To further identify key AOM communities, we investigated the archaeal community by pyrosequencing of 16S rRNA genes. In general, MCG_c of the phylum Crenarchaeota

dominated the archaeal communities, accounting for up to 99.2 % (see Fig. S2). *Methanomicrobia* of the phylum Euryarchaeota, which contains the order *Methanosarcinales*, was more abundant in the upper depths of the MV sediment cores than the lower depths (see Table S3 and Fig. S2). For clarifying the phylogenetic position within the class *Methanomicrobia* including both methanogens and methanotrophs, phylogenies of the three most dominant (more than 1 % of all archaeal sequences) *Methanomicrobia* OTUs (c116, c1698, and c1784), were inferred from 16S rRNA gene sequences (Supplementary Information Table S3). The OTU c116 represented 2.5–14.1 % and 0.2–6.7 % of the *archaeal* sequences at core depths of 0.0–0.2 m in MV282 and 0.1–1.1 m in MV420, respectively, whereas this OTU was less than 0.2 % at MV740 (Supplementary information Table S3). The OUT c1698 accounted for more than 1 % of the archaeal sequences at the surface of MV282 but was absent at other MVs. The OTU c1784 accounted for 1.2–6.8 % and 3.7–14.9 % of the archaeal sequences at core depths of 0.0–0.2 m in MV282 and 0.4–0.6 m in MV740, respectively. In contrast, this OTU was rarely detected at all depths of MV420, except for at the depth of 0.7 m. The OTUs c116 and c 1698 belonged to ANME-3 archaeal lineage and the OUT c1784 formed a cluster with sequences of ANME-2c, a distict lineage of *Methanosarcinales* (Fig. 5). Hence, the occurrence of AOM related to ANME-2 and ANME-3 inferred from the AOM-related lipid data could be confirmed by 16S rRNA-specific analysis for ANME groups, while ANME-1 sequences were not retrieved from the Beaufort Sea MVs investigated here.

4.3 Mechanism controlling microbial communities at Beaufort Sea mud volcanoes

16S rRNA signatures from the Beaufort Sea MVs revealed the presence of AOM related to archaeal ANME-2, albeit in relatively low proportions (Fig. 5). The ANME-2 can be

divided into three subgroups, ANME-2a, ANME-2b, and ANME-2c (e.g. Orphan et al., 2001; Knittel et al., 2005). In the Beaufort Sea MVs, the ANME-2c subgroup was detected (Fig. 5). A previous study at Hydrate Ridge (Cascadia margin off Oregon, USA) showed that ANME-2c was dominant at symbiotic clam *Calyptogena* sites, accounting for >75 % of the total ANME-2, whereas ANME-2a was the most abundant at sulfide-oxidizing bacterium *Beggiatoa* sites, accounting for up to 80 % (Knittel et al., 2005). Other studies at Hydrate Ridge showed that the fluid flows and the methane fluxes from the seafloor were substantially weaker at *Calyptogena* sites than at *Beggiatoa* sites (e.g. Tryon et al., 1999; Sahling et al., 2002). Hence, it seems that ANME-2c has a preferential niche in habitats with lower methane fluxes.

The thermal gradients in our study area (see Paull et al., 2015) were substantially higher in the MVs (517.7 mK/m in MV282, 557.9 mK/m in MV420, and 104.3 mK/m in MV740) than in the reference site (28.9 mK/m). In general, high geothermal gradients were observed where methane emission activities were high, as reported at Dvurechenskii MV (Feseker et al., 2009) and Haakon Mosby MV (Kaul et al., 2006). Accordingly, among the MV sites, the methane flux appeared to be the highest at the MV420 site. Indeed, we found a lower abundance of ANME-2c in MV420 than in MV282 and MV740 (Fig. 5, see also Table S3). The MV740 site had the lowest thermal gradient of the MV sites, and thus probably the lowest methane flux, which is consistent with the presence of the gas hydrate flake at 230 cm in the MV740 sediment core (see Fig. 1D, Paull et al., 2015). At this MV site, ANME-2c occurred at a deeper core depth (0.3–0.7 m) than at the MV282 site (0.0–0.3 m, see also Table S3). This might be linked to the lower methane flux at the MV740 site than at the MV282 site, resulting in penetration of sulfate to deeper sediment depths. Notably, at active MV sites, the sulfate penetration depth can be limited to the upper 2-cm sediment layers (cf. Niemann et al.,

2006).

Besides ANME-2c, 16S rRNA gene analyses also revealed the presence of ANME-3 (see Table S3). Notably, ANME-3 occurred in MV420 whereas ANME-2c was almost abscent. However, ANME-3 was abscent in MV740 while ANME-2c was present. As mentioned above, the thermal gradient was higher in MV420 than in other MVs. Previously, ANME-3 was reported as a dominant cluster of archaeal sequences at Haakon Mosby Mud Volcano located in Barents Sea at the water depth of 1,250 m associated with bacterial *Beggiatoa* mats, whereas ANME-2 was more closely related to the sites of siboglinid tubeworm colonies (Niemann et al., 2006). Typically, the fluid flow rates were higher at the sites of the *Beggiatoa* mats than the siboglinid tubeworm colonies at Haakon Mosby Mud Volcano (Niemann et al., 2006). Accordingly, it seems that ANME-3 could thrive better in a setting with higher thermal gradients than ANME-2c.

5 Conclusions

Integrated biogeochemical and nucleic acid analyses were performed for three sediment cores retrieved from the active MVs in the Beaufort Sea. $\delta^{13}C_{TOC}$ values of three sediment cores were restricted to a very narrow range of –26.4±0.6 ‰, without a negative isotopic excursion. Crocetane and PMI were not detected, whereas archaeol and hydroxyarchaeols were present in all investigated samples along with non-isoprenoid DGD (If). The isoprenoidal GDGTs were dominated by GDGT-0 and crenarchaeol, with relatively low abundances of GDGT-1 and GDGT-2. The $\delta^{13}C$ values of archaeol, BPs, and the non-isoprenoid DGD (If) were enriched relative to the $\delta^{13}C_{CH4}$ value. These findings suggest that the contribution of AOM-related biomass to sedimentary TOC was generally negligible in the Beaufort Sea MVs investigated. However, the $\delta^{13}C$ values of *sn*-2- and *sn*-3-hydroxyarchaeol

were more depleted than the $\delta^{13}C_{CH4}$ values, indicative of the presence of AOM. The ratio of *sn*-2-hydroxyarchaeol relative to archaeol and the archaeal 16S rRNA gene sequence results supported the involvement of ANME-2c and ANME-3 in AOM at Beaufort Sea MVs. Accordingly, it appears that CH_4 is, to a limited extent, being oxidized in the Beaufort Sea MVs investigated. Given that our gravity coring system failed to recover the uppermost surface sediments, preventing us from detecting the most active AOM occurrences in the Beaufort Sea MVs, further studies should investigate the undisturbed uppermost surface sediments to investigate the diversity and distribution of AOM communities and to characterize their habitats in the Beaufort Sea MV systems, for instance, using ROV pushcores.

Author contribution

JHK, DHL and YML prepared the manuscript with contributions from all co-authors. DHL, YML, YKJ, JHK, and KHS designed the experiments and were responsible for the analysis. YGK provided thermal gradient data.

Competing interests

The authors declare that they have no conflict of interest.

Acknowledgments

We would like to thank the captain and crew of R/V ARAON for their safe and skillful operation of the ship during the cruise. This study was supported by the KOPRI project (PM17050) funded by the Ministry of Oceans and Fisheries (MOF), and by a National Research Foundation of Korea (NRF) grants funded by the Ministry of Science and ICT

(MSIT) (NRF-2016M1A5A1901769, PN17081; NRF-2016R1A2B3015388, PN17100). We also thank Y. Chikaraishi and M. Kaneko for their help in isotope measurements of biphytanes during a short stay in JAMSTEC, Japan. We are grateful to J.-K. Gal, S. Kang, and D. Kim for their analytical assistance in the laboratory at Hanyang University.

References

Beal, E. J., House, C. H., Orphan, V. J.: Manganese- and iron-dependent marine methane oxidation, Science, 325, 184-187, 2009.

Blasco, K., White, M., Campbell, P., Oickle, E., Burke, R., and Blasco, S. M.: 2004 Beaufort Sea Mapping Program – Geological Analysis, Draft Report prepared by Canadian Seabed Research Ltd. for the Geological Survey of Canada, 2006.

Blasco, S., Bennett, R., Brent, T., Burton, M., Campbell, P., Carr, E., Covill, R., Dallimore, S., Davies, E., Hughes-Clarke, J., Issler, D., MacKillop, K., Mazzotti, S., Patton, E., Shearer, J., White, M.: 2010 state of knowledge: Beaufort Sea seabed geohazards associated with offshore hydrocarbon development, Geological Survey of Canada Open File 6989, 340 pp, 2013.

Blumenberg, M., Seifert, R., Reitner, J., Pape, T. and Michaelis, W.: Membrane lipid patterns typify distinct anaerobic methanotrophic consortia, Proc. Natl. Acad. Sci., 101, 11111–11116, 2004.

Boetius, A., Ravenschlag, K., Schubert, C. J., Rickert, D., Widdel, F., Gieseke, A., Amann, R., Jørgensen, B. B., Witte, U. and Pfannkuche, O.: A marine microbial consortium apparently mediating anaerobic oxidation of methane, Nature, 407, 623–626, 2000.

Bradley, A. S., Hayes, J. M. and Summons, R. E.: Extraordinary 13C enrichment of diether lipids at the Lost City Hydrothermal Field indicates a carbon-limited ecosystem,

Geochim. Cosmochim. Acta, 73, 102–118, 2009.

Campbell, P., Carr, E., Beaton, F., and Blasco, S. M.: 2009 Beaufort Sea Seabed Mapping Program – Operations Report, Draft Report prepared by Canadian Seabed Research Ltd. for the Geological Survey of Canada, 2009.

Chevalier, N., Bouloubassi, I., Birgel, D., Cremiere, A., Taphanel, M. H. and Pierre, C.: Authigenic carbonates at cold seeps in the Marmara Sea (Turkey): A lipid biomarker and stable carbon and oxygen isotope investigation, Mar. Geol., 288, 112–121, 2011.

Chevalier, N., Bouloubassi, I., Birgel, D., Taphanel, M. H. and López-García, P.: Microbial methane turnover at Marmara Sea cold seeps: A combined 16S rRNA and lipid biomarker investigation, Geobiology, 11, 55–71, 2013.

Chevalier, N., Bouloubassi, I., Stadnitskaia, A., Taphanel, M. H. and Sinninghe Damsté, J. S.: Lipid biomarkers for anaerobic oxidation of methane and sulphate reduction in cold seep sediments of Nyegga pockmarks (Norwegian margin): Discrepancies in contents and carbon isotope signatures, Geo-Marine Lett., 34, 269–280, 2014.

De Rosa, M. and Gambacorta, A.: The Lipids of archaebacteria, Prog. Lipid Res., 27, 153–175, 1988.

Edgar, R. C., Haas, B. J., Clemente, J. C., Quince, C. and Knight, R.: UCHIME improves sensitivity and speed of chimera detection, Bioinformatics, 27, 2194–2200, 2011.

Elvert, M., Hopmans, E. C., Treude, T., Boetius, a. and Suess, E.: Spatial variations of methanotrophic consortia at cold methane seeps: Implications from a high-resolution molecular and isotopic approach, Geobiology, 3, 195–209, 2005.

Etminan, M., Myhre, G., Highwood, E. J. and Shine, K. P.: Radiative forcing of carbon dioxide, methane, and nitrous oxide: A significant revision of the methane radiative forcing, Geophys. Res. Lett., 43, 12,614–12,623, 2016.

Felden, J., Wenzhöfer, F., Feseker, T. and Boetius, A.: Transport and consumption of oxygen and methane in different habitats of the Håkon Mosby Mud Volcano (HMMV), Limnol. Oceanogr., 55, 2366–2380, 2010.

Felsenstein, J.: Evolutionary Trees from DNA Sequences : A Maximum Likelihood Approach, J. Mol. Evol., 17, 368–376, 1981.

Ferrante, G., Ekiel, I., Patel, G. B. and Sprott, G. D.: A novel core lipid isolated from the aceticlastic methanogen, *Methanothrix concilii* GP6, Biochim. Biophys. Acta - Lipids Lipid Metab., 963, 173–182, 1988.

Feseker, T., Pape, T., Wallmann, K., Klapp, S. A., Schmidt-Schierhorn, F. and Bohrmann, G.: The thermal structure of the Dvurechenskii mud volcano and its implications for gas hydrate stability and eruption dynamics, Mar. Pet. Geol., 26, 1812–1823, 2009.

Feseker, T., Boetius, A., Wenzhofer, F., Blandin, J., Olu, K., Yoerger, D. R., Camilli, R., German, C. R. and De Beer, D.: Eruption of a deep-sea mud volcano triggers rapid sediment movement, Nat. Commun., 5, 1–8, 2014.

Grosse, G., and Jones, B. M.: Spatial distribution of pingos in northern Asia, The Cryosphere, 5, 13–33, 2011.

Haese, R. R., Meile, C., Van Cappellen, P. and De Lange, G. J.: Carbon geochemistry of cold seeps: Methane fluxes and transformation in sediments from Kazan mud volcano, eastern Mediterranean Sea, Earth Planet. Sci. Lett., 212, 361–375, 2003.

Haroon, M. F., Hu, S., Shi, Y., Imelfort, M., Keller, J., Hugenholtz, P., Yuan, Z., Tyson, G. W.,: Anaerobic oxidation of methane coupled to nitrate reduction in a novel archaeal lineage, Nature, 500, 567-570, 2013.

Himmler, T., Birgel, D., Bayon, G., Pape, T., Ge, L., Bohrmann, G. and Peckmann, J.: Formation of seep carbonates along the Makran convergent margin , northern Arabian

Sea and a molecular and isotopic approach to constrain the carbon isotopic composition of parent methane, Chem. Geol., 415, 102–117, 2015.

Hinrichs, K. U. and Boetius, A.: The anaerobic oxidation of methane: new insights in microbial ecology and biogeochemistry, edited by G. Wefer, D. Billett, D. Hebbeln, B. B. Jørgensen, M. SCHLÜ TER, and T. VAN WEERING, Springer-Verlag, Berlin, Germany, 2002.

Hovland, M., Jensen, S. and Fichler, C.: Methane and minor oil macro-seep systems - Their complexity and environmental significance, Mar. Geol., 332–334, 163–173, 2012.

Hwang, K., Oh, J., Kim, T. K., Kim, B. K., Yu, D. S., Hou, B. K., Caetano-Anollés, G., Hong, S. G. and Kim, K. M.: CLUSTOM: A Novel Method for Clustering 16S rRNA Next Generation Sequences by Overlap Minimization, PLoS One, 8, e62623, 2013.

Huguet, C., Hopmans, E. C., Febo-Ayala, W., Thompson, D. H., Sinninghe Damsté, J. S. and Schouten, S.: An improved method to determine the absolute abundance of glycerol dibiphytanyl glycerol tetraether lipids, Org. Geochem., 37, 1036–1041, 2006.

James, R. H., Bousquet, P., Bussmann, I., Haeckel, M., Kipfer, R., Leifer, I., Niemann, H., Ostrovsky, I., Piskozub, J., Rehder, G., Treude, T., Vielstädte, L., Greinert, J.: Effects of climate change on methane emissions from seafloor sediments in the Arctic Ocean: A review, Limnol. Oceanogr., 61, 283–299, 2016.

Kaneko, M., Kitajima, F. and Naraoka, H.: Stable hydrogen isotope measurement of archaeal ether-bound hydrocarbons, Org. Geochem., 42, 166–172, 2011.

Kaul, N., Foucher, J. P. and Heesemann, M.: Estimating mud expulsion rates from temperature measurements on Håkon Mosby Mud Volcano, SW Barents Sea, Mar. Geol., 229, 1–14, 2006.

Kim, J., Lee, D., Yoon, S., Jeong, K., Choi, B. and Shin, K.: Chemosphere Contribution of

petroleum-derived organic carbon to sedimentary organic carbon pool in the eastern Yellow Sea (the northwestern Pacific), Chemosphere, 168, 1389–1399, 2017.

Kim, O. S., Cho, Y. J., Lee, K., Yoon, S. H., Kim, M., Na, H., Park, S. C., Jeon, Y. S., Lee, J. H., Yi, H., Won, S. and Chun, J.: Introducing EzTaxon-e: A prokaryotic 16s rRNA gene sequence database with phylotypes that represent uncultured species, Int. J. Syst. Evol. Microbiol., 62, 716–721, 2012.

Knittel, K., Lösekann, T., Boetius, A., Kort, R., Amann, R. and Lo, T.: Diversity and Distribution of Methanotrophic Archaea at Cold Seeps Diversity and Distribution of Methanotrophic Archaea at Cold Seeps, Appl. Environ. Microbiol., 71, 467–479, 2005.

Knittel, K. and Boetius, A.: Anaerobic oxidation of methane: Progress with an unknown process, Annu. Rev. Microbiol., 63, 311–334, 2009.

Koga, Y., Nishihara, M., Morii, H. and Akagawa-Matsushita, M.: Ether polar lipids of methanogenic bacteria: Structures, comparative aspects, and biosyntheses, Microbiol. Rev., 57, 164–182, 1993.

Koga, Y., Morii, H., Akagawa-Matsushita, M. and Ohga, M.: Correlation of Polar Lipid Composition with 16S rRNA Phylogeny in Methanogens. Further Analysis of Lipid Component Parts, Biosci. Biotechnol. Biochem., 62, 230–236, 1998.

Koga, Y. and Morii, H.: Recent Advances in Structural Research on Ether Lipids from Archaea Including Comparative and Physiological Aspects, Biosci. Biotechnol. Biochem., 69, 2019–2034, 2005.

Kopf, A. J.: Significance of mud volcanism, Rev. Geophys., 40, 2–46, 2002.

Kushwaha, S. C. and Kates, M.: 2, 3-Di-O-phytanyl-sn-glycerol and prenols from extremely halophilic bacteria, Phytochemistry, 17, 2029–2030, 1978.

Liu, X., Lipp, J. S. and Hinrichs, K.-U.: Distribution of intact and core GDGTs in marine

sediments, Org. Geochem., 42, 368–375, 2011.

Lösekann, T., Robador, A., Niemann, H., Knittel, K., Boetius, A. and Dubilier, N.: Endosymbioses between bacteria and deep-sea siboglinid tubeworms from an Arctic Cold Seep (Haakon Mosby Mud Volcano, Barents Sea), Environ. Microbiol., 10, 3237–3254, 2008.

Mulicka, J., Ferdelman, T. G., Polerecky, L., Franzke, D., Wegner, G., Schmid, M., Lieberwirth, I., Wagner, M., Widdel, F., Kuyper, M. M. M.: Zero-valent sulphur is a key intermediate in marine methane oxidation, Nature, 491, 541–546, 2012.

Niemann, H., Elvert, M., Hovland, M., Orcutt, B., Judd, A., Suck, I., Gutt, J., Damm, E., Finster, K. and Boetius, A.: Methane emission and consumption at a North Sea gas seep (Tommeliten area), Biogeosciences, 2, 1197–1241, 2005.

Niemann, H., Lösekann, T., de Beer, D., Elvert, M., Nadalig, T., Knittel, K., Amann, R., Sauter, E. J., Schlüter, M., Klages, M., Foucher, J. P. and Boetius, A.: Novel microbial communities of the Haakon Mosby mud volcano and their role as a methane sink, Nature, 443, 854–858, 2006.

Niemann, H. and Elvert, M.: Diagnostic lipid biomarker and stable carbon isotope signatures of microbial communities mediating the anaerobic oxidation of methane with sulphate, Org. Geochem., 39, 1668–1677, 2008.

Oh, J., Kim, B. K., Cho, W. S., Hong, S. G. and Kim, K. M.: PyroTrimmer: A software with GUI for pre-processing 454 amplicon sequences, J. Microbiol., 50, 766–769, 2012.

Omoregie, E. O., Niemann, H., Mastalerz, V., Lange, G. J. De, Stadnitskaia, A., Mascle, J., Foucher, J. and Boetius, A.: Microbial methane oxidation and sulfate reduction at cold seeps of the deep Eastern Mediterranean Sea, Mar. Geol., 261, 114–127, 2009.

Orphan, V. J., Hinrichs, K., Iii, W. U., Paull, C. K., Taylor, L. T., Sylva, S. P., Hayes, J. M.

and Delong, E. F.: Comparative Analysis of Methane-Oxidizing Archaea and Sulfate-Reducing Bacteria in Anoxic Marine Sediments, Appl. Environ. Microbiol., 67, 1922–1934, 2001.

Pancost, R. D., Sinninghe Damsté, J. S., Lint, S. D., van der Maarel, M. J. E. C., Gottschal, J. C. and Shipboard Scientific Party: Biomarker evidence for widespread anaerobic methane oxidation in Mediterranean sediments by a consortium of methanogenic archaea and bacteria, Appl Environ. Microbiol., 66, 1126–1132, 2000.

Pancost, R. D., Bouloubassi, I., Aloisi, G. and Sinninghe Damsté, J. S.: Three series of non-isoprenoidal dialkyl glycerol diethers in cold-seep carbonate crusts, Org. Geochem., 32, 695–707, 2001a.

Pancost, R. D., Hopmans, E. C., Sinninghe Damsté, J. S. and Scientific Party, the M. S.: Archaeal lipids in mediterranean cold seeps: Molecular proxies for anaerobic methane oxidation, Geochim. Cosmochim. Acta, 65, 1611–1627, 2001b.

Pancost, R. D., McClymont, E. L., Bingham, E. M., Roberts, Z., Charman, D. J., Hornibrook, E. R. C., Blundell, A., Chambers, F. M., Lim, K. L. H. and Evershed, R. P.: Archaeol as a methanogen biomarker in ombrotrophic bogs, Org. Geochem., 42, 1279–1287, 2011.

Paull, C. K., Ussler, W., Dallimore, S. R., Blasco, S. M., Lorenson, T. D., Melling, H., Medioli, B. E., Nixon, F. M. and McLaughlin, F. A.: Origin of pingo-like features on the Beaufort Sea shelf and their possible relationship to decomposing methane gas hydrates, Geophys. Res. Lett., 34, 1–5, 2007.

Paull, C. K., Dallimore, S. R., Caress, D. W., Gwiazda, R., Melling, H., Riedel, M., Jin, Y. K., Hong, J. K., Kim, Y.-G., Graves, D., Sherman, A., Lundsten, E., Anderson, K., Lundsten, L., Villinger, H., Kopf, A., Johnson, S. B., Clarke, J. H., Blas, S., Conway, K., Neelands, P., Thomas, H. and Cote, M.: Active mud volcanoes on the continental slope of the

Canadian Beaufort Sea, Geochem. Geophys. Geosyst., 16, 1541–1576, 2015.

Reeburgh, W. S.: Oceanic Methane Biogeochemistry, Chem. Rev., 107, 486–513, 2007.

Sahling, H., Rickert, D., Lee, R. W., Linke, P. and Suess, E.: Macrofaunal community structure and sulfide flux at gas hydrate deposits from the Cascadia convergent margin, NE Pacific, Mar. Ecol. Prog. Ser., 231, 121–138, 2002.

Saint-ange, F., Kuus, P., Blasco, S., Piper, D. J. W., Hughes, J. and Mackillop, K.: Multiple failure styles related to shallow gas and fluid venting, upper slope Canadian Beaufort Sea, northern Canada, Mar. Geol., 355, 136–149, 2014.

Schouten, S., Wakeham, S. G., Hopmans, E. C. and Sinninghe Damsté, J. S.: Biogeochemical evidence that thermophilic archaea mediate the anaerobic oxidation of methane, Appl. Environ. Microbiol., 69, 1680–1686, 2003.

Serov, P., Vadakkepuliyambatta, S., Mienert, J., Patton, H., Portnov, A., Silyakova, A., Panieri, G., Carroll, M. L., Carroll, J., Andreassen, K. and Hubbard, A.: Postglacial response of Arctic Ocean gas hydrates to climatic amelioration, Proc. Natl. Acad. Sci. USA, 114, 6215–6220, 2017.

Shearer, J. M., Macnab, R. F., Pelletier, B. R. and Smith, T. B.: Submarine Pingos in the Beaufort Sea, Science, 174, 816–818, 1971.

Sprott, G. D., Dicaire, C. J., Choquet, C. G., Patel, G. B., Ekiel, I. and Dennis, G.: Hydroxydiether Lipid Structures in Hydroxydiether Lipid Structures in Methanosarcina Methanococcus voltaet, Appl. Environ. Microbiol., 59, 912–914, 1993.

Stadnitskaia, A, Ivanov, M. K. and Sinninghe Damsté, J. S.: Application of lipid biomarkers to detect sources of organic matter in mud volcano deposits and post-eruptional methanotrophic processes in the Gulf of Cadiz, NE Atlantic, Mar. Geol., 255, 1–14, 2008a.

Stadnitskaia, A., Nadezhkin, D., Abbas, B., Blinova, V., Ivanov, M. K. and Damste, J. S. S.: Carbonate formation by anaerobic oxidation of methane: Evidence from lipid biomarker and fossil 16S rDNA, Geochim. Cosmochim. Acta, 72, 1824–1836, 2008b.

Tamura, K., Stecher, G., Peterson, D., Filipski, A. and Kumar, S.: MEGA6: Molecular evolutionary genetics analysis version 6.0, Mol. Biol. Evol., 30, 2725–2729, 2013.

Tryon, M. D., Brown, K. M., Torres, M. E., Tréhu, A. M., McManus, J. and Collier, R. W.: Measurements of transience and downward fluid flow near episodic methane gas vents, Hydrate Ridge, Cascadia, Geology, 27, 1075–1078, 1999.

Walker, D. A., M. D. Walker, K. R. Everett, and Webber, P. J.: Pingos of the Prudhoe Bay Region, Alaska, Arct. Alp. Res., 17, 321–336, 1985.

Wegner, G., Niemann, H., Elvert, M., Hinrich, K. U., Boetius, A.: Assimilation of methane and inorganic carbon by microbial communities mediating the anaerobic oxidation of methane, Environ. Microbiol., 10, 2287–2298, 2008.

Weijers, J. W. H., Lim, K. L. H., Aquilina, A., Sinninghe Damsté, J. S. and Pancost, R. D.: Biogeochemical controls on glycerol dialkyl glycerol tetraether lipid distributions in sediments characterized by diffusive methane flux, Geochem. Geophys. Geosyst., 12, Q10010, 2011.

Whiticar, M. J.: Carbon and hydrogen isotope systematics of bacterial formation and oxidation of methane, Chem. Geol., 161, 291–314, 1999.

Werne, J. P., Haese, R. R., Zitter, T., Aloisi, G., Bouloubassi, I., Heijs, S., Fiala-Médioni, A., Pancost, R. D., Sinninghe Damsté, J. S., de Lange, G., Forney, L. J., Gottschal, J. C., Foucher, J. P., Mascle, J. and Woodside, J.: Life at cold seeps: A synthesis of biogeochemical and ecological data from Kazan mud volcano, eastern Mediterranean Sea, Chem. Geol., 205, 367–390, 2004.

Wuebbles, D. J. and Hayhoe, K.: Atmospheric methane and global change, Earth-Sci. Rev., 57, 177–210, 2002.

Zhang, C. L., Pancost, R. D., Sassen, R., Qian, Y. and Macko, S. A.: Archaeal lipid biomarkers and isotopic evidence of anaerobic methane oxidation associated with gas hydrates in the Gulf of Mexico, Org. Geochem., 34, 827–836, 2003.

Zhang, Y. G., Zhang, C. L., Liu, X.-L., Li, L., Hinrichs, K.-U. and Noakes, J. E.: Methane Index: A tetraether archaeal lipid biomarker indicator for detecting the instability of marine gas hydrates, Earth Planet. Sci. Lett., 307, 525–534, 2011.

Figure captions

Fig. 1. (A) Map showing the study area (red box) with inset regional map of Alaska and northwestern Canada modified from Paull et al. (2015). (B) Map showing the three mud volcano (MV) locations on the upper slope of the Beaufort Sea. (C) Detailed bathymetric maps showing the locations of sediment cores ARA05C-10-GC (MV282), ARA05C-01-GC (MV420), and ARA05C-18-GC (MV740). (D) Lithology of the three sediment cores investigated.

Fig. 2. Examples of GC-MS chromatograms of polar fractions obtained from sediment cores (A) ARA05C-10-GC (MV282): core depth 0.1 m, (B) ARA05C-01-GC (MV420): core cepth 0.7 m, and (C) ARA05C-18-GC (MV740): core cepth 0.8 m. Solid triangles denote *n*-alcohols.

Fig. 3. Vertical profiles of selected lipid biomarkers (archaeol, hydroxyarchaeol, and DGD (If)) obtained from sediment cores (A) ARA05C-10-GC (MV282), (B) ARA05C-01-GC (MV420), and (C) ARA05C-18-GC (MV740). Grey hatched bars indicate gas gaps in sediment layers.

Fig. 4. HPLC/APCI-MS base peak chromatograms of polar fractions obtained from sediment cores (A) ARA05C-10-GC (MV282), (B) ARA05C-01-GC (MV420), and (C) ARA05C-18-GC (MV740). Note that the Roman numerals (I, II, III, IV and V) refer to GDGT-0, GDGT-1, GDGT-2, GDGT-3, and crenarchaeol, respectively. The Arabic numbers in GDGT-0, GDGT-1, GDGT-2, and GDGT-3 indicate the number of cyclopentane rings within the biphytane chains.

Biogeosciences Discuss., https://doi.org/10.5194/bg-2018-91
Manuscript under review for journal Biogeosciences
Discussion started: 4 April 2018

Fig. 5. Phylogenetic tree based on 16S rRNA showing the relationships of methanomicrobial sequences recovered in this study with selected reference sequences of the domain Euryarchaeota. The phylogenetic tree was inferred by the maximum-likelihood method. Filled circles indicate bootstrap values higher than 70 % based on 1,000 replications. The scale bar indicates evolutionary distance of 0.05 substitutions per site.

Biogeosciences Discuss., https://doi.org/10.5194/bg-2018-91
Manuscript under review for journal Biogeosciences
Discussion started: 4 April 2018

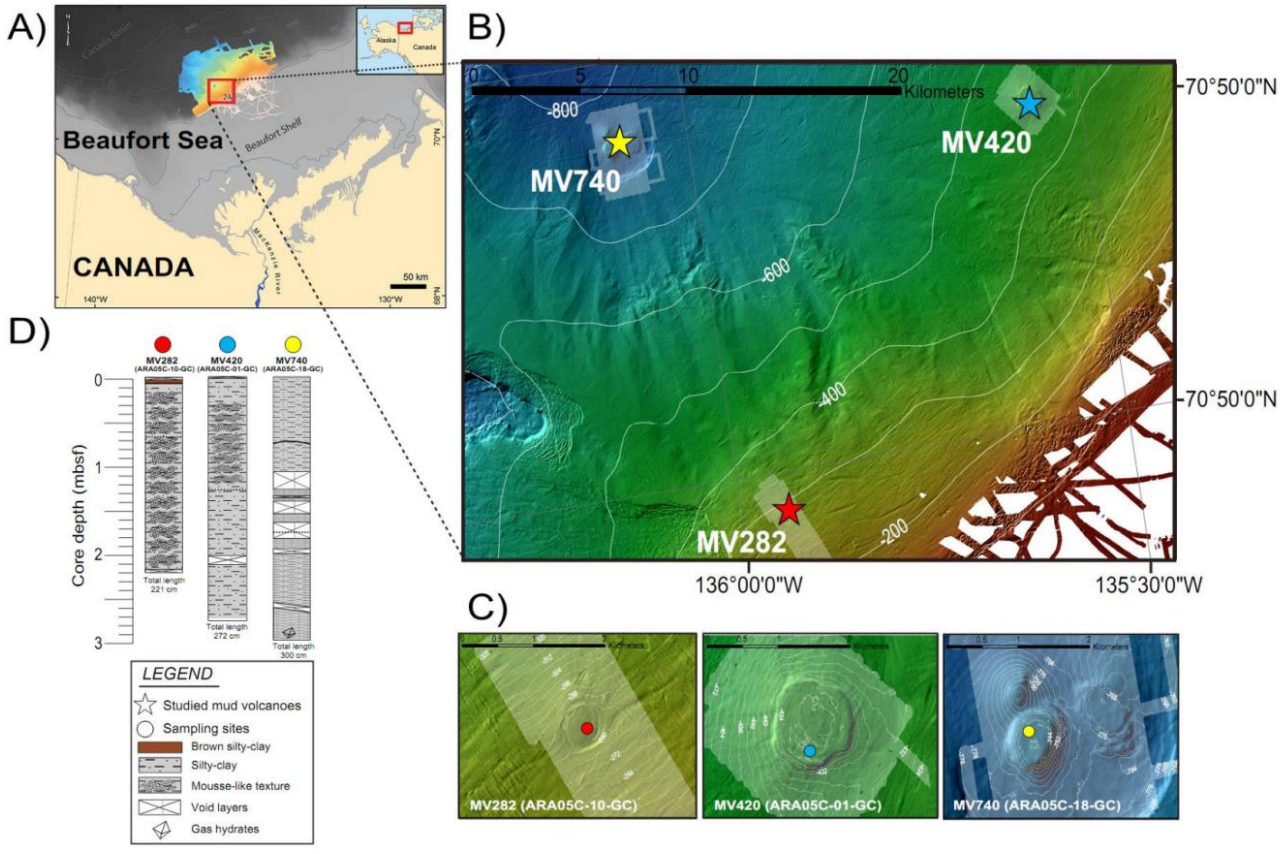

Fig. 1

Biogeosciences Discuss., https://doi.org/10.5194/bg-2018-91
Manuscript under review for journal Biogeosciences
Discussion started: 4 April 2018

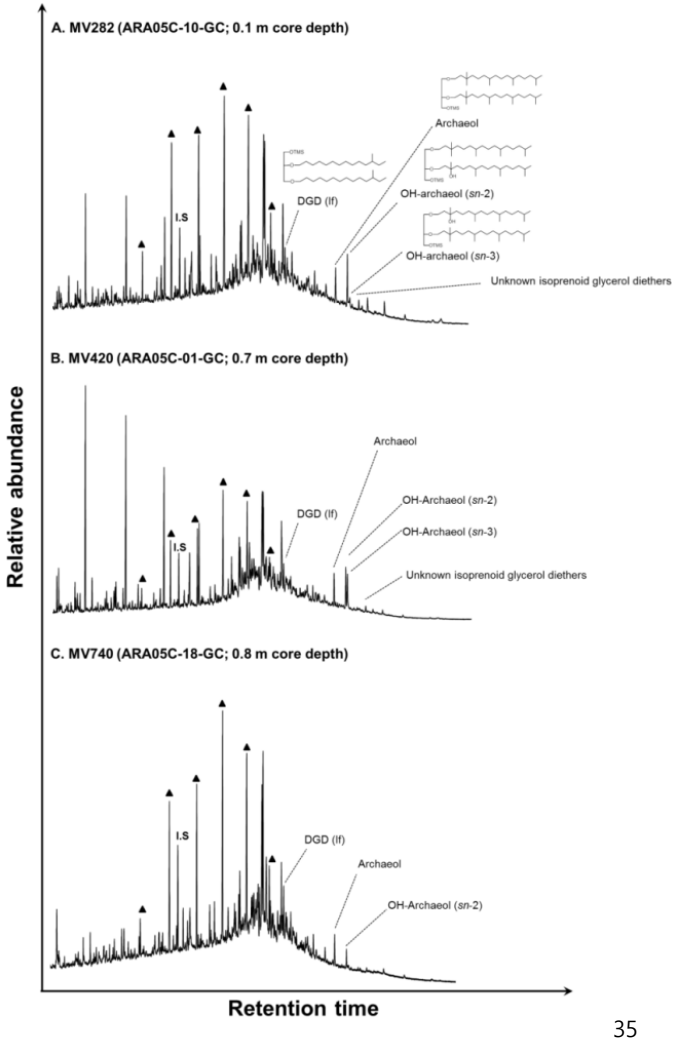

Fig. 2

Biogeosciences Discuss., https://doi.org/10.5194/bg-2018-91
Manuscript under review for journal Biogeosciences
Discussion started: 4 April 2018

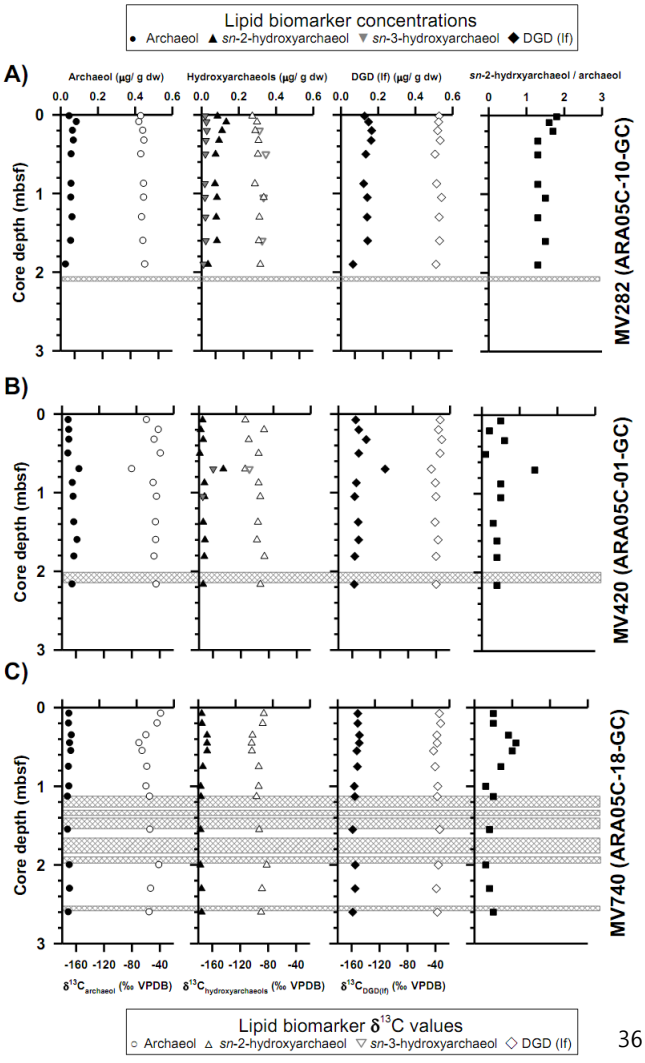

Fig. 3

Biogeosciences Discuss., https://doi.org/10.5194/bg-2018-91
Manuscript under review for journal Biogeosciences
Discussion started: 4 April 2018

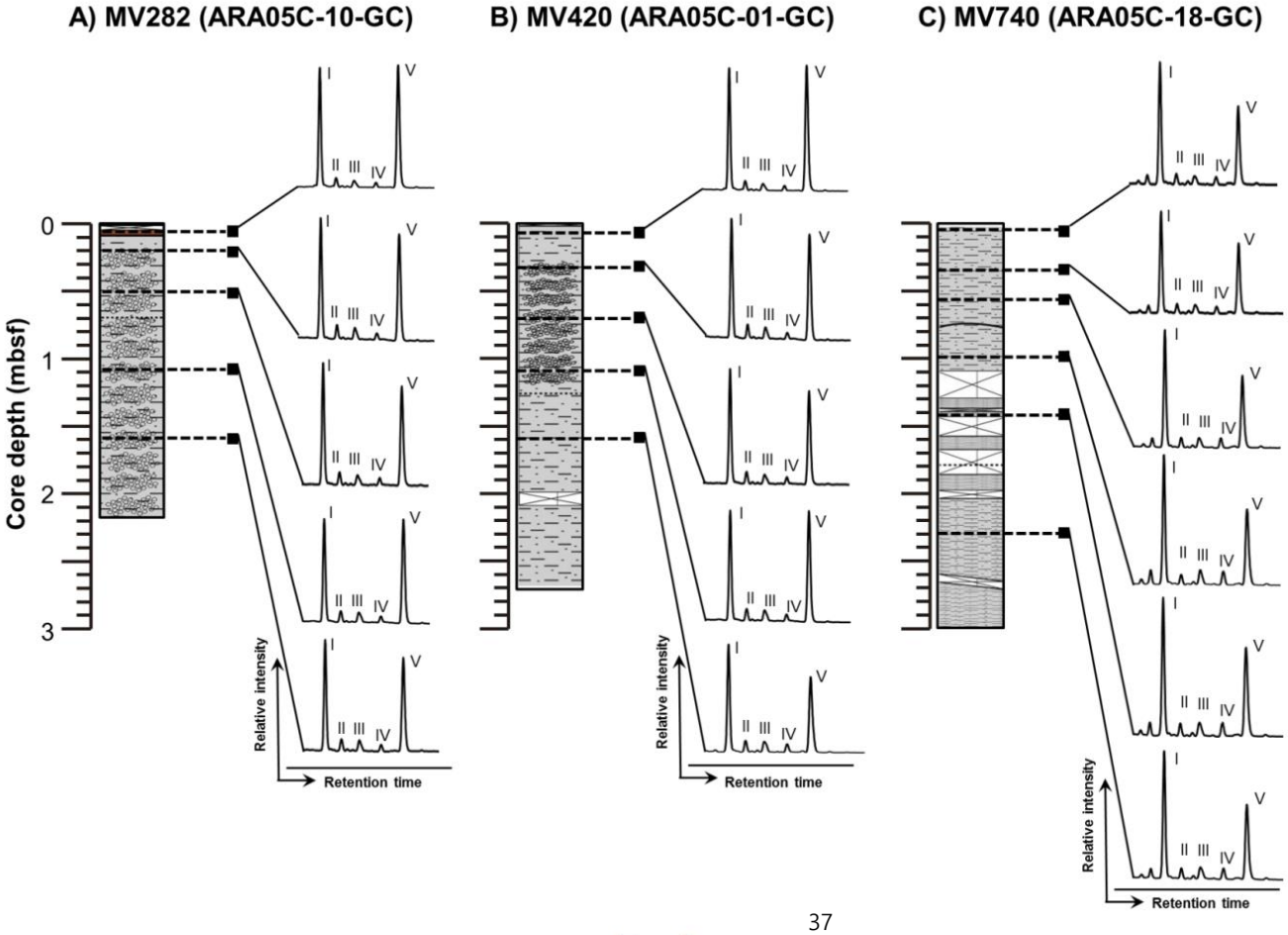

Fig. 4

Biogeosciences Discuss., https://doi.org/10.5194/bg-2018-91
Manuscript under review for journal Biogeosciences
Discussion started: 4 April 2018

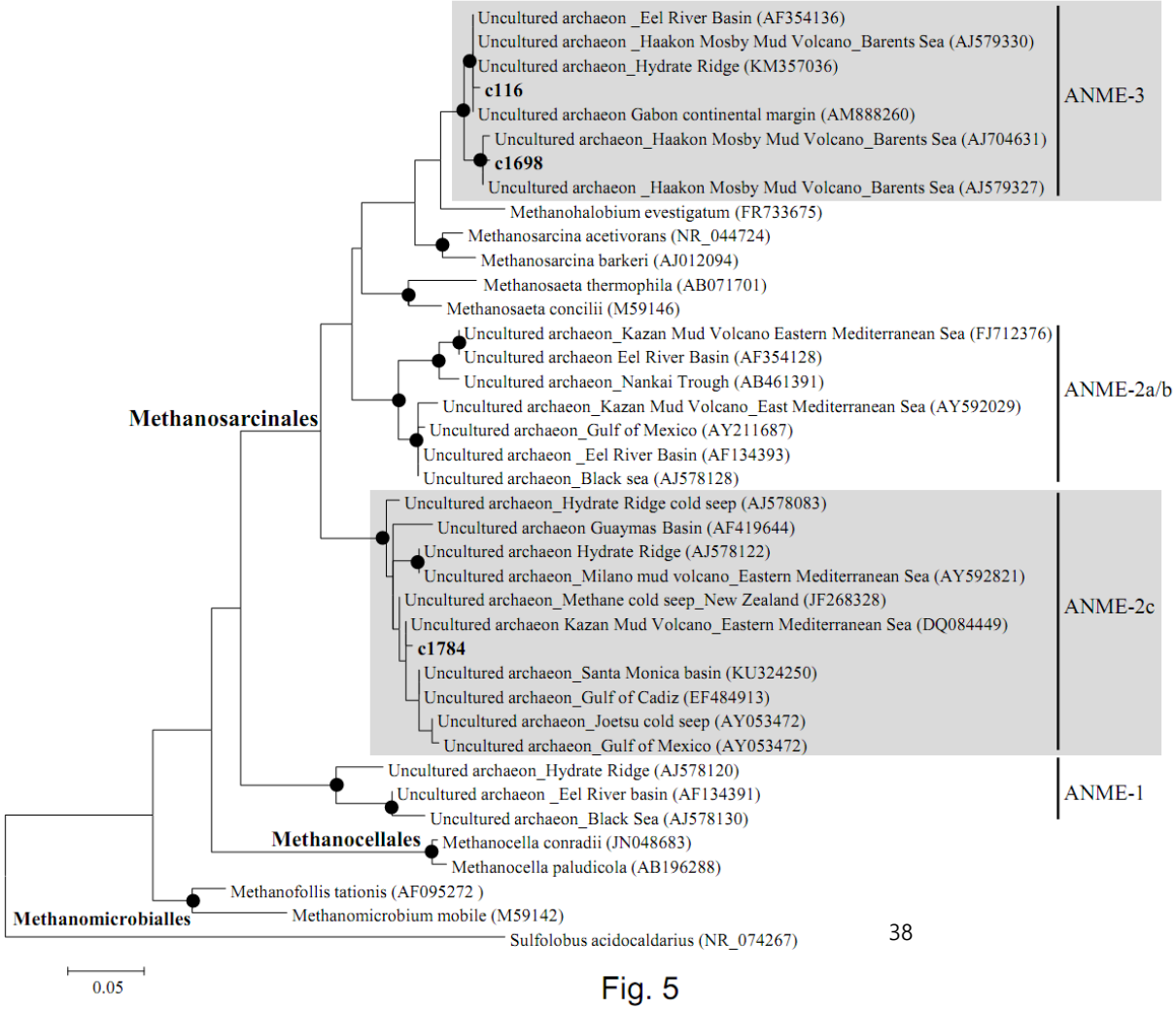

Fig. 5